Adaptive optics point spread function reconstruction directly from target data

Szymon Gladysz

Fraunhofer Institute of Optronics, System Technologies and Image Exploitation, Gutleuthausstr. 1, 76275 Ettlingen, Germany

Abstract: Reconstruction of point spread function (PSF) using information from the wavefront sensor is a classic problem in adaptive optics. Although the theory and methods for this task have been in use for the last twenty years, implementation and application of the classic PSF reconstruction still proves difficult and will become even more formidable for future adaptive optics systems. Here we present an alternative solution which does not require any extra information from the wavefront sensor, nor does it rely on knowledge of the turbulence profile; the method requires a sequence of images of the same object.

OCIS codes: (010.1330) Atmospheric turbulence, (010.1080) Active or adaptive optics

1. Introduction

In imaging through turbulence it is almost always beneficial to post-process (e.g. deconvolve) the observations, even if they were taken with adaptive optics (AO). We say "almost" because when a mismatched PSF is used for deconvolution the final image will in the most optimistic scenario not improve, and in most cases it will look worse than the raw data. Especially in the astronomical community the task of measuring the PSF simultaneously with the scientific observations has been given a lot of attention [1-3]. The problem also has relevance for surveillance & reconnaissance [4] as well as imaging of space-based assets [5].

The classic PSF reconstruction of Veran et al. [1] has only been partly successful as a wide-spread tool for astronomical imaging. One problem with this approach, aside from the requirement to model all random processes in the telescope and its instrumentation, is that it requires measurement of the vertical profile of turbulence at the time of the observations. This could be done with a balloon probe or a turbulence profiler. Nevertheless, this solution involves associated logistics, costs and problems with scalability to more complicated AO systems. Automatic modeling of multi-conjugate AO, especially with laser guide stars, in the era of extremely large telescopes would be a formidable task.

Here we propose to tackle the problem using two object-cancelling transformations applied to multi-frame imagery. Use is made of approximate expressions for partially-developed speckle contrast and speckle skewness due to Yaitskova et al. [6]. With these expressions it is possible to extract average PSF from images of any objects, taken either with AO or at long wavelengths and/or with small apertures whereby phase standard deviation of the incoming wavefront is less than π (scenario of military reconnaissance).

2. Theory

We start with the realization that the optical transfer function (OTF), **H**, is a speckle [5]:

$$\mathbf{H}(\vec{u}) = \frac{1}{N}\sum_{i=1}^{N} e^{j\left(\theta(\xi_i,\eta_i)-\theta(\xi_i+\bar{\lambda}\, z u_X,\eta_i+\bar{\lambda}\, z u_Y)\right)} \tag{1}$$

where ξ,η are the pupil-plane coordinates, $\bar{\lambda}$ is the average wavelength of the observations, z is the distance from the exit pupil to the image plane, N is the number of OTF cells in the area of overlap [5] and θ's are the phases – identically distributed random variables. Normalization factor $1/N$ has been chosen in accordance with [6] but it will not play a role in the final expressions.

Note that because phases are random the OTF also has to be random, even for long exposures. OTF would have the same statistics as amplitude while models for intensity are applicable to power spectral density $|\mathbf{H}|^2$. With this realization one can proceed to write down the expressions for non-central moments of $|\mathbf{H}|^2$ [6]:

$$\left\langle |\mathbf{H}|^2 \right\rangle = \frac{1}{N^2}\left(N + N_1 M_1^2\right), \tag{2}$$

$$\left\langle |\mathbf{H}|^4 \right\rangle = \frac{1}{N^4}\left[N + 2N_1 + 4(N_1+N_2)M_1^2 + N_1M_2^2 + N_3M_1^4 + 2N_2M_1^2M_2\right],$$
$$\left\langle |\mathbf{H}|^6 \right\rangle = \frac{1}{N^6}\{N + 9N_1 + 6N_2 + 3(5N_1+15N_2+6N_3)M_1^2 + 9(2N_3+N_4)M_1^4 + N_5M_1^6 + 3(2N_1+3N_2)M_2^2 + N_1M_3^2 + 9N_3M_1^2M_2^2 + 2\left[3N_2M_1M_2M_3 + N_3M_1^3M_3 + 3(4N_2+3N_3)M_1^2M_2 + 3N_4M_1^4M_2\right]\}, \quad \text{(2, contd.)}$$

where M_m is the characteristic function of $\theta(\xi_i,\eta_i) - \theta(\xi_i + \bar{\lambda}\, zu_X, \eta_i + \bar{\lambda}\, zu_Y)$ and $N_n = N!/(N-n-1)!$. For normally-distributed phase, M_m are expressed in terms of the structure function of the phase D_θ: $M_m = \exp\left(-\frac{D_\theta(\bar{\lambda}\, zu_X, \bar{\lambda}\, zu_Y)m^2}{2}\right)$.

Contrast C (standard deviation divided by the mean value) and skewness S of $|\mathbf{H}|^2$ can be computed using their definitions:

$$C \equiv \frac{\sqrt{\left\langle |\mathbf{H}|^4 \right\rangle - \left\langle |\mathbf{H}|^2 \right\rangle^2}}{\left\langle |\mathbf{H}|^2 \right\rangle}$$
$$S \equiv \frac{\left\langle |\mathbf{H}|^6 \right\rangle - 3\left\langle |\mathbf{H}|^4 \right\rangle\left\langle |\mathbf{H}|^2 \right\rangle + 2\left\langle |\mathbf{H}|^2 \right\rangle^3}{\left(\left\langle |\mathbf{H}|^4 \right\rangle - \left\langle |\mathbf{H}|^2 \right\rangle^2\right)^{\frac{3}{2}}} \quad (3)$$

The resulting expressions are very long but fortunately approximations for large N have been derived [6]:

$$C \approx \sqrt{\frac{2}{N}}\frac{1 - \left\langle |\mathbf{H}|^2 \right\rangle}{\sqrt{\left\langle |\mathbf{H}|^2 \right\rangle}}, \quad N \gg 1$$
$$S \approx \frac{1}{\sqrt{2N}}\frac{3 - 6\left\langle |\mathbf{H}|^2 \right\rangle - \left\langle |\mathbf{H}|^2 \right\rangle^2}{\sqrt{\left\langle |\mathbf{H}|^2 \right\rangle}}, \quad N \gg 1 \quad (4)$$

3. Method

The imaging equation for a true object $o(\vec{x})$ convolved with a PSF $h(\vec{x})$, giving the recorded image $i(\vec{x})$ is:

$$i(\vec{x}) = o(\vec{x}) \otimes h(\vec{x}) \quad (5)$$

where the symbol $\vec{x}$ corresponds to two-dimensional focal-plane coordinate. Equation (5), transformed into Fourier domain, squared and averaged over M images, becomes:

$$\left\langle |I(\vec{u})|^2 \right\rangle_M = |O(\vec{u})|^2 \left\langle |H(\vec{u})|^2 \right\rangle_M \quad (6)$$

When one computes contrast and skewness of the resulting quantity the object disappears:

$$C\left(\left\langle |I(\vec{u})|^2 \right\rangle_M\right) = C\left(\left\langle |H(\vec{u})|^2 \right\rangle_M\right) \quad \text{and} \quad S\left(\left\langle |I(\vec{u})|^2 \right\rangle_M\right) = S\left(\left\langle |H(\vec{u})|^2 \right\rangle_M\right) \quad (7)$$

Note that all static terms disappear from the result, i.e. also telescope OTF will be removed. Therefore in order to obtain realistic PSF one has to multiply the result of the method again by the telescope OTF, preferably one which

includes also static errors of the optics. Looking at Equation (4) we see that we obtained two equations with two unknowns: the modulation transfer function $|\mathbf{H}|$ and the number of OTF cells *N*. One can now proceed to calculate modulation transfer function $|\mathbf{H}|$ for any object being imaged. Beforehand, one last simplification in Equation (4) is used:

$$\left\langle \left|\mathbf{H}(\vec{u})\right|^2 \right\rangle = \frac{1}{N}\left[1+(N-1)\exp\left(-D_\theta(\bar{\lambda}\, zu_X, \bar{\lambda}\, zu_Y)\right)\right] \approx \exp\left(-D_\theta(\bar{\lambda}\, zu_X, \bar{\lambda}\, zu_Y)\right) \approx \left|\left\langle \mathbf{H}(\vec{u}) \right\rangle\right|^2, \quad N >> 1 \qquad (8)$$

This simplification is not strictly necessary; After all, one still has two equations with two unknowns if it is not applied. On the other hand it greatly simplifies calculations.

4. Experiment

For the tests a sequence of 4000 short exposure images (t_{exp} = 22 ms) of a single bright star taken with the 3-m Shane Telescope at the Lick Observatory was used. For details of data reduction, the reader is directed to [7]. Images were taken in K-band (2.2 μm) with AO on and the resulting Strehl ratio was 53%. Power spectra were computed for each image and subsequently contrast and skewness values of each frequency component were computed, i.e. statistical quantities were averaged over time. The azimuthally-averaged results of applying Equation (4) to the resulting contrast and skewness images are shown in the left panel of Figure 1. In the right panel we show the corresponding images of PSFs. These first results are very encouraging. The true and estimated MTFs overlap and structure of the PSF is well represented (note the AO correction zone, roughly 14 pixels in size, in panel **c**). The results are more than satisfactory given that the fiber PSF was taken around two years after the first observations.

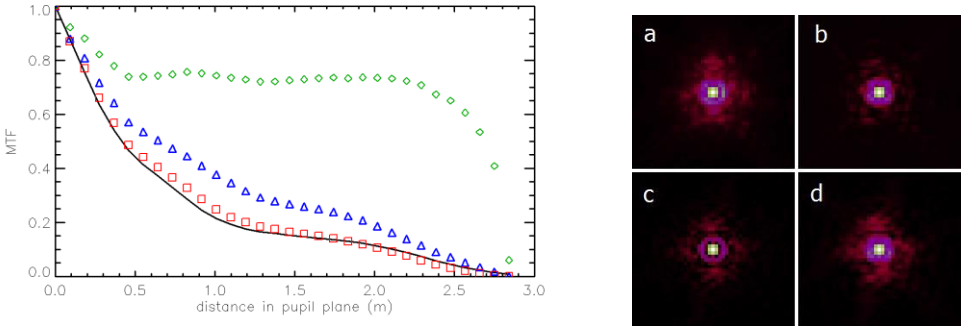

Fig. 1. Illustration of the method's performance. Left: Black line: ground truth, i.e. the MTF corresponding to the observations. Green diamonds: estimated MTF of the turbulence AO-residuals only. Blue triangles: estimated AO MTF (green diamonds) multiplied by the perfect, diffraction-limited MTF. Red squares: AO MTF multiplied by the MTF containing the telescope and static error terms (taken from a fiber PSF). Right: (a) ground truth – in this case real PSF, (b) fiber PSF (no turbulence, only static errors), (c) result of PSF reconstruction after inclusion of the perfect, diffraction-limited MTF, (d) result of PSF reconstruction after inclusion of the information from the fiber PSF.

5. Conclusions

We have introduced a novel was of extracting a PSF from sequence of images of arbitrary objects. The method is applicable to astronomical imaging with AO and to imaging with small apertures and/or long wavelengths. Especially interesting will be the application of the new approach to estimation of spatially-varying PSF in single-conjugate AO. We posit that the method should work with less than 100 images. There is also nothing preventing the use of the method with long exposures: the only thing that will change will be then the number of random phasors *N* which will correspondingly increase. Practical issue might arise in that both contrast and skewness diminish towards zero when *N* increases (see Equation (4)). This might lead to degeneracy of the solution. This and other issues will be explored in the future.

ACKNOWLEDGEMENTS: This material is based upon work supported by the Air Force Office of Scientific Research, Air Force Material Command, USAF under Award No. FA9550-14-1-0244.

6. References

[1] Jean-Pierre Veran, Francois Rigaut, Henri Maitre, and Daniel Rouan, "Estimation of the adaptive optics long-exposure point-spread function using control loop data," JOSA A 14, (1997).
[2] Laurent Jolissant, Hervé Carfantan, and Eric Anterrieu, "Exploring the impact of PSF reconstruction errors on the reduction of astronomical adaptive optics based data," Proc.SPIE, 7015, 159 (2008).
[3] Laurent Jolissaint, Julian Christou, Peter Wizinowich, and Eline Tolstoy, "Adaptive optics point spread function reconstruction: lessons learned from on-sky experiment on Altair/Gemini and pathway for future systems", Proc. SPIE 7736, Adaptive Optics Systems II, 77361F (2010).
[4] Szymon Gladysz and Roberto Baena Gallé, "Comparison of image restoration algorithms in the context of horizontal-path imaging," Proc. SPIE 8355, 83550X-1-12 (2012).
[5] Szymon Gladysz, Roberto Baena Gallé, Robert Johnson, and Lee Kann, "Image reconstruction of extended objects: demonstration with the Starfire Optical Range 3.5m telescope," Proceedings of SPIE, Volume 8535, 85350M-1-13 (2012).
[6] Natalia Yaitskova, Michael Esselborn, and Szymon Gladysz, "Statistical moments of the Strehl ratio," Proc. SPIE 8447, 84475Y (2012).
[7] Szymon Gladysz, Julian C. Christou, and Michael Redfern, "Characterization of the Lick adaptive optics point spread function," Proc. SPIE 6272, 62720J (2006).